Relaxation in the ^1A_u state of glyoxal. I. Collision-free lifetimes of single vibrational levels

R. A. Beyer*, P. F. Zittel, and W. C. Lineberger†

Department of Chemistry, University of Colorado, Boulder, Colorado 80302

Joint Institute for Laboratory Astrophysics, University of Colorado and National Bureau of Standards, Boulder, Colorado 80302

(Received 17 December 1974)

Collision free lifetimes are reported for 26 single vibrational levels of the ^1A_u state of glyoxal (CHOCOH). A nitrogen laser-pumped tunable dye laser is used to excite primarily single vibronic levels of glyoxal in the pressure range 10^{-5}–10^{-1} Torr. The resulting fluorescence can either be spectrally resolved to provide single vibronic level observation or the entire ^1A_u emission can be detected. The fluorescence is time-resolved with 100 nsec resolution, and two or more decades of decay are typically observed. A detailed discussion of the apparatus and techniques is presented. Evidence is presented for very rapid rotation and vibration collisional energy transfer, and implications of these effects on extrapolated zero-pressure lifetimes are discussed. By observing an entire vibronic band, effects of rapid rotational redistribution on observed loss rates can be minimized, and thus by varying the total glyoxal pressure, one can determine single vibronic level loss rate constants. Such data are presented for 26 vibronic levels, with cross sections which range from gas kinetic to seven times faster than gas kinetic. These collisional loss rate constants are dominated by vibrational relaxation; an observable but less important loss channel is collision induced intersystem crossing. Implications of these data are discussed.

I. INTRODUCTION

For many years experimental investigations of radiationless transitions in polyatomic molecules were limited to the study of absorption and emission spectra of condensed media.[1] The more recent recognition of the intramolecular nature of these transitions has led to studies of isolated vapor phase molecules.[2–8] In two of the early studies of the behavior of isolated molecules, Schlag and von Weyssenhoff[2] excited beta-naphthylamine using a light source with a spectral width of 10 000 cm^{-1} and Laor and Ludwig[3] excited naphthalene with a spectral bandwidth of almost 15 000 cm^{-1}, which excited three singlet states. While these experiments show good agreement with general predictions of radiationless transitions theory, in both cases the excitation bandpass is too great to obtain information about the decay of individual vibrational levels.

Von Weyssenhoff and Kraus[4] have observed vibronic effects in the lifetimes and quantum yields of aniline vapor with excitation from 3000 to 2725 Å with a 2.7 Å bandpass. However, the extensive overlap of the absorption bands prevented the extraction of detailed information of single vibronic levels. Utilizing narrower spectral bandwidth, Yeung and Moore[5] studied radiationless transitions and subsequent photochemistry following the excitation of single vibronic levels of formaldehyde. Rice and his co-workers[6] have used narrow band excitation and photon counting detection to study in detail the effects of symmetry and energy of single vibronic levels in radiationless transitions of benzene and several derivatives. Other recent single vibronic level excitation studies have included those of Frad *et al.*[7] and Pocius and Yardley.[8]

Glyoxal (CHOCOH) has two spectroscopically observable low-lying electronic states, ^1A_u and ^3A_u, in addition to the ^1A_g ground state. The ^1A_u–^1A_g transition, with 0–0 band near 4550 Å, has been studied extensively[9] in absorption and emission in the visible, in microwave absorption via electron diffraction, and in high resolution infrared studies. The vibrational frequencies obtained from this previous work are shown in Table I. Quenching rate constants and a collision-free lifetime have been reported[10,11] for the vibrationless level of the ^1A_u state following excitation of glyoxal vapor with a tunable dye laser.

There are three main features of the absorption and emission spectra of the ^1A_u–^1A_g transition. The first is that both spectra are relatively uncomplicated and well-identified. The second feature is the addition of sequence bands of the low energy (127 cm^{-1}) torsional mode, ν_7, onto all other bands in absorption at room temperature and onto all but the lowest pressure emission spectra. Since the frequency of this mode is 233 cm^{-1} in the ^1A_u excited state, one may readily separate any of the ν_7 sequence bands from the 0–0 band.

The third important feature of the glyoxal spectra is that the 8_1^0 band in emission, and to a lesser extent the 8_0^1 band in absorption, are unusually strong transitions. This effect arises from the fact that although the ^1A_u–^1A_g transition is symmetry allowed, it is relatively weak, with oscillator strength $f \sim 4\times10^{-5}$.[12] Since glyoxal has C_{2h} point symmetry, B_u–A_g transitions are also allowed. Therefore the b_g symmetry of ν_8 is correct ($b_g \times A_u = B_u$) for a vibronic interaction that is significant due to the weakness of the ^1A_u–^1A_g transition.[13] It has been verified[14] that the 0–0 band is a type C band while the 8_1^0 band is a type $A+B$ band, as predicted from the orientation of the dipole components.

In the studies reported in this paper, narrow band excitation by a tunable dye laser and observation of emission resolved by a spectrometer have been used to measure the lifetimes of 26 individual vibrational levels of the ^1A_u state of glyoxal molecules. Also reported are

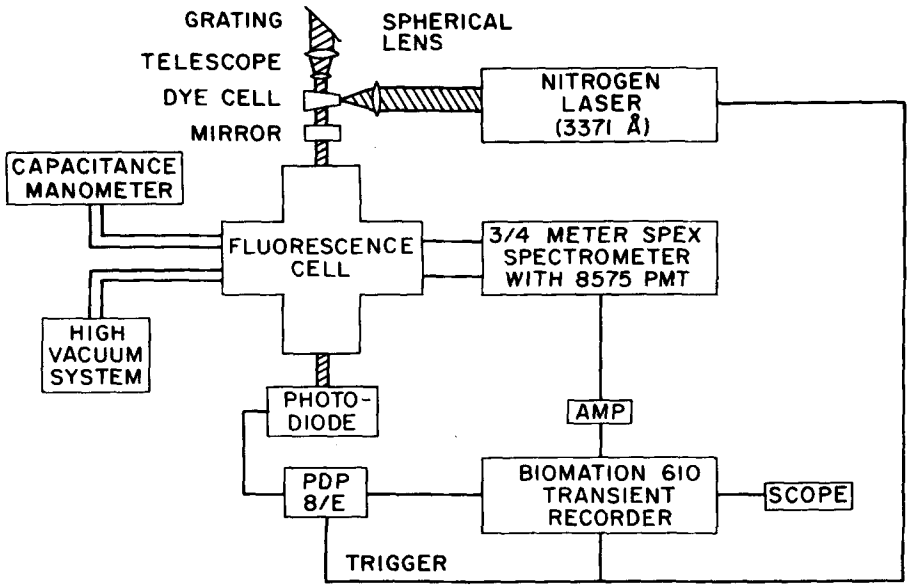

FIG. 1. Block diagram of experimental apparatus for time and energy resolved fluorescence studies.

the rate constants for quenching of these levels by ground state glyoxal molecules.

II. APPARATUS

A block diagram of the apparatus used in this experiment is shown in Fig. 1. The excitation source is a tunable dye laser transversely pumped by a 300 kW nitrogen laser.[15] The basic design of the dye laser system is similar to that of Hänsch.[16] It consists of a dye cell containing the flowing dye, a ten-power telescope which expands the beam onto a diffraction grating (1800 lines/mm blazed at 5000 Å), and a partially reflective dielectric coated output mirror ($R \sim 4\%$ for most of this work).

The dye cell used here is of a unique design. A machined stainless steel block is used to hold a quartz or sapphire light pipe, antireflection coated windows, and to provide access to the active region for flowing the dye, as shown in Fig. 2. The 3-mm diameter light pipe is bonded to the block with a thin ring of epoxy. The output of the nitrogen laser is focused onto the top of the light pipe with a spherical lens; the dye concentration is chosen such that the 337 nm pump radiation is absorbed in about 0.2 mm of dye solution below the light pipe. The organic dyes and scintillators used are given in Table II. The output of the dye laser is typically 0.1–0.5 mJ in a pulse of $\sim 10^{-8}$ sec duration. The linewidth was about 0.5 Å (FWHM) for most of the work described here.

The dye laser output light is directed to the fluorescence cell, a 3-cm diameter stainless steel cross with removable 7056 pyrex windows. This cell connects to a standard glass high vacuum system pumped by a trapped oil diffusion pump. The base pressure of the system is typically 5×10^{-7} Torr. Glyoxal pressure over the range of 1 mTorr to 1 Torr is measured with a capacitance manometer. The manometer head is held at a slightly elevated temperature to ensure stability and reduce condensation. A small correction is made for thermal transpiration[17] when significant.

TABLE I. Vibrational frequencies of glyoxal[a] (cm^{-1}).

Symmetry species	Vibration	Ground state ^1A_g	Excited states ^1A_u	^3A_u
a_g	ν_1 C–H stretch	2843	2809	
	ν_2 C–O stretch	1745	1391	1458
	ν_3 C–H rock	1338		
	ν_4 C–C stretch	1065	955	963
	ν_5 C–C–O bend	550	509	502
a_u	ν_6 C–H wag	801		
	ν_7 torsional	127	233	234
b_g	ν_8 C–H wag	1048	735	
b_u	ν_9 C–H stretch	2835		
	ν_{10} C–O stretch	1732		
	ν_{11} C–H stretch	1312		
	ν_{12} C–C–O bend	339	380	391

[a]Reference 14 and references therein.

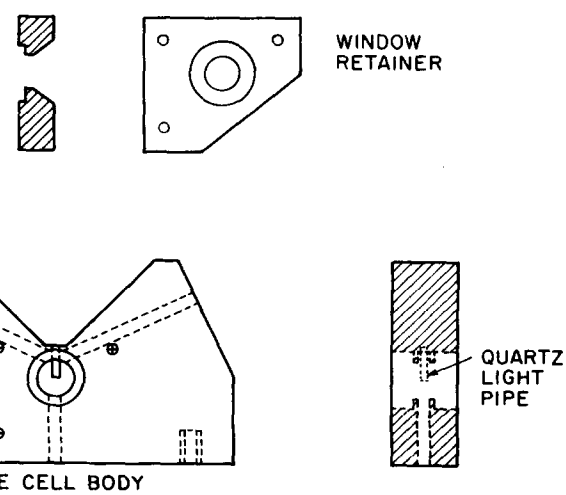

FIG. 2. The dye cell used in the tunable dye laser. Nitrogen laser light is focused onto the top of the quartz light pipe and absorbed by the dye solution at the lower surface of the light pipe.

TABLE II. Organic dyes and scintillators used in the spectral region 3550–5300 Å.

Material/Solvent	Wavelength region (Å)
Phenylbiphenyloxadiazole (PBD)/toluene	3550–3850
Alpha-naphthylphenyloxazole (α-NPO)/toluene	3900–4140
1,4-bis[2-(5-phenyloxazolyl)]benzene (POPOP)/toluene	4100–4215
1,4-bis[2-(4-methyl-5-phenyloxazolyl)]benzene (Dimethyl-POPOP)/toluene	4140–4380
7-diethylamino-4-methylcoumarin/benzene	4200–4480
7-diethylamino-4-methylcoumarin/ethanol	4360–5050
Brilliant sulphaflavine/ethanol	4800–5300

Scattered laser light is minimized by focusing the laser output to about 1-mm diameter in the region of the cell where emission is viewed. Diaphrams with 0.5 cm holes are placed inside the cell away from the viewing region to reduce scattered light. As a result of the focusing of the excitation light, transitions such as the 0–0 and 7_1^1 are saturated under typical experimental conditions. In any instance where one desired that excitation be linear with laser intensity, the beam was defocused and attenuated to achieve this condition. In no case has any dependence on laser power density been found for any lifetime or rate constant in this glyoxal work.

The emission from the excited glyoxal may be observed in two ways. For experiments requiring moderately high wavelength resolution, the fluorescence is imaged into an $f/6.8$, 0.75-m spectrometer with dispersion of about 10 Å/mm in the spectral region of interest. Since slit widths as small as 50 μm are used, the slits are perpendicular to the line of emission to avoid effects due to diffusion from the field of view.[18] The optics used to image the emission provide a field of view which is approximately a 1-cm radius cylindrical region centered on the line of excitation. Under normal operating conditions, no scattered laser light is detected through the spectrometer when observing more than a few angstroms away from the excitation wavelength. The light through the spectrometer is detected by an RCA 8575 photomultiplier tube.

For viewing a larger portion of the emission than is convenient through the spectrometer, an RCA 1P28/V1 photomultiplier tube is mounted at the window of the cross opposite the spectrometer. Since some scattered laser light was detected with this photomultiplier, care was taken to avoid saturation of either the photomultiplier tube or subsequent electronics.

The output voltage of either photomultiplier tube is amplified by a dc-coupled preamplifier with a fixed gain of 50 and a risetime for full output of about 100 nsec. Both the 8575 photomultiplier and preamplifier are rigorously shielded from the radio frequency interference generated by the nitrogen laser discharge. The amplified signal is digitized with 100 nsec resolution by a model 610 Biomation transient recorder, with frequency response to 2.5 MHz. The limited (6 bit) resolution of the transient recorder results in quantization noise being the dominant source of noise after coherent summation of a number of fluorescence decays. This source of uncertainty can be reduced and the dynamic range of the transient recorder extended to at least 9 bits by adding white noise to the fluorescence signal at the input to the transient recorder. Two data runs are then required to obtain the fluorescence decay: The first is a normal signal run, and the second is a light blocked run which defines the zero signal level to a precision greater than the 6 bit resolution of the recorder.

The digitized data are summed coherently by a PDP 8/E computer that controls the timing of the experiment. A typical data run consists of the sum of emission from several hundred laser pulses at a repetition rate of 10–15 Hz. Data from 50 consecutive runs can be stored on a magnetic tape cassette for later analysis. Least-squares fits for simple exponential behavior are done directly by the data acquisition program.

Glyoxal was prepared[19] by oxidizing ethylene with selenium dioxide in the presence of phosphorous pentoxide at about 200 °C. It was purified by distillation and stored in an evacuated cell at dry ice temperature. To test the useable limits of a single sample of glyoxal, the fluorescence lifetime of a sample isolated in the cell by a greaseless valve was studied as a function both of excitation energy and time after filling the cell. At a pressure of about 100 mTorr of glyoxal, with excitation only to low-lying levels of the ^1A_u state, the observed lifetime increases by a few percent over a period of several hours, due to the slow polymerization of glyoxal on the walls of the cell. Excitation to levels of the ^1A_u state with over 1000 cm^{-1} of excess vibrational energy results in substantially increased loss of glyoxal molecules, apparently due to photochemical destruction. These observations are consistent with evidence for two loss mechanisms at higher pressures previously reported by Norrish and Griffiths.[20]

III. PROCEDURE

The optimum excitation wavelength for a desired absorption band was determined either from a low resolution absorption spectrum or from the calculated band origin. In most cases, when observing with a 10 Å bandpass, the apparent fluorescence lifetime did not change as the excitation wavelength was varied over a few angstroms in the region of the predicted wavelength. This result is not unexpected since both absorption and emission bands are approximately 10 Å wide.

Using an excitation bandwidth of 0.5 Å, it is clear that more than one vibrational level is being excited at most wavelengths. One may scan the spectrometer with fixed excitation and observe simple exponential decays with different lifetimes at wavelengths that can be identified as emission from different vibrational levels of the ^1A_u state. The main reasons for excitation of more than one vibrational level with a 0.5 Å bandwidth are the substantially populated hot bands due to the 127 cm^{-1} ground state frequency of the torsional mode and the fact that the rotational envelopes of the vibrational bands of glyoxal are approximately as wide as the separation of band centers. An important example of a hot band is a significant emission near 4450 Å (7_0^2) when exciting the 0–0 band near 4550 Å. This wavelength not only excites the 0–0 band, but also the 7_4^2 band, which has an appreciable

thermal population in the lower state.

It was found early in this study that the observed collisional quenching rate of glyoxal by other glyoxal molecules is a function of both excitation and observation bandwidths. This dependence is attributed to rotational relaxation. As an example, one may excite in the 0–0 band with a 0.5 Å bandwidth laser (which excites several hundred rotational levels) and observe the 5_1^0 emission band, which has the same rotational structure as the 0–0 band. At pressures near 10 mTorr the 5_1^0 emission band consists of a narrow peak about 0.5 Å wide with a lower intensity normal 5_1^0 band contour under it. As the excitation wavelength is changed within the 0–0 absorption envelope this emission peak follows exactly, a clear indication that rotational relaxation is incomplete before the level has largely decayed radiatively. Under these conditions, if one observes the 5_1^0 emission peak with 0.5 Å bandpass the apparent quenching slope is about 18 $\mu sec^{-1} \cdot Torr^{-1}$, compared with a value of 5.8 $\mu sec^{-1} \cdot Torr^{-1}$ with the same excitation and observation with 10 Å resolution. In either case the same zero-pressure intercept is obtained from a Stern–Volmer quenching plot. The faster rate clearly includes rotational relaxation while the slower rate is due only to vibrational and electronic relaxation. These data provide direct evidence of very rapid collisional rotational relaxation ($\sigma > 100$ Å^2) in the ^1A_u state of glyoxal. This process will be discussed in more detail in a subsequent publication.[21]

With fixed wavelength observation, rotational relaxation can similarly produce changes in observed lifetime with variations in excitation wavelength over an absorption band. For example, with a 2 Å observation bandpass centered on the 8_1^0 emission band, the measured lifetime varies by a factor of 2 as excitation is varied across the 0–0 absorption band, at 10 mTorr glyoxal pressure. As the observational bandpass is increased, the lifetime variations decrease. At a 10 Å bandpass, there are no systematic variations in the lifetime as the excitation wavelength is varied as above, and we conclude that enough of the emission is detected to avoid effects due to rotational relaxation within the same band. In some cases the low pressure lifetime data were retaken with about 1 Å resolution of the emission to minimize possible effects of overlapping bands.

In a related experiment, the lifetime of the vibrationless level of the ^1A_u state was determined at 10^{-5} Torr with an excitation band width of 0.2 Å and observational bandpass of 10 Å. No variations greater than 1% were found in the lifetime of this level as the laser was varied over the 0–0 absorption envelope. This result indicates that the ^1A_u collision free lifetime is not a strong function of rotational levels accessible in the excitation.

A simple procedure was used to isolate the emission from the desired level. Fluorescence was first observed at a wavelength where emission from that level should be strongest, while exciting the strongest transition to that level. If more than one emission band or other than single exponential decay was observed at low pressure, other combinations of absorption and emission bands were used to verify that emission from the desired level was in fact being observed. In this manner it was possible in most cases to observe emission from single vibronic levels, although for some levels it was necessary to observe a band other than the strongest one in order to maximize the fraction of fluorescence originating from the desired level. This procedure minimizes error due to the overlap of emission bands.

Glyoxal pressures for these data were typically in the range 2–25 mTorr. Above 25 mTorr rapid vibrational relaxation causes nonexponential decay behavior for many of the observed levels. The signal levels in this lower pressure range are more than adequate to insure that the emission decay is a single exponential over at least three lifetimes.

After subtraction of the baseline from a data run, a least-squares semilogarithmic fit is made to the time resolved fluorescence over the region of single exponential decay to obtain the time constant (inverse lifetime) at each pressure. These fits were typically made over two decades or more of decay for the results presented here. Typical pressure dependences of the loss rates are shown in Fig. 3, and are seen to be linear. Using simple Stern–Volmer analysis,[22] a linear least-squares fit is made to these quenching plots to obtain a zero-pressure lifetime from the intercept and a collisional quenching rate constant from the slope. In the cases of the vibrationless level, the 5^1 level, and the 8^1 level, the lifetimes were also measured at pressures of 10^{-5} Torr.

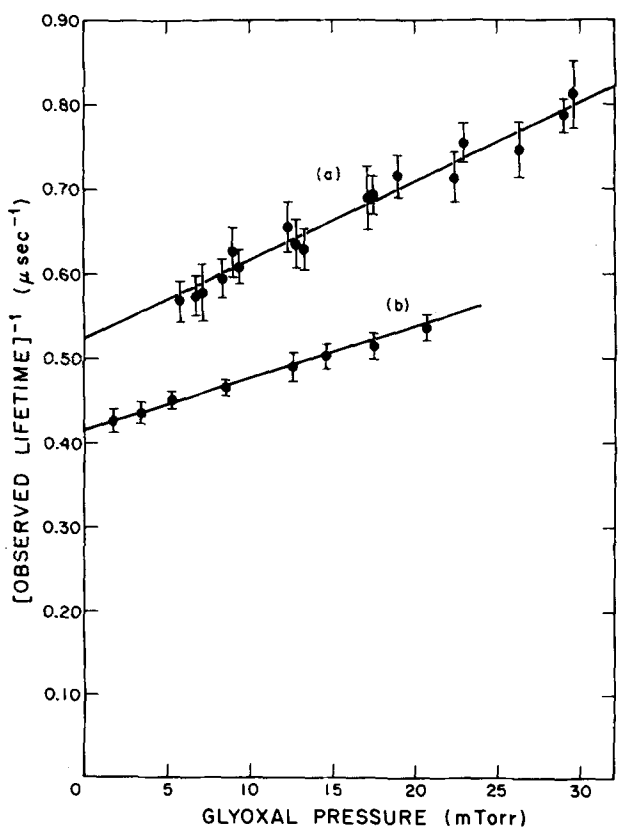

FIG. 3. Quenching of two typical vibrational levels of the ^1A_u state by ground state glyoxal molecules. Shown are (a) the $5^1 7^2$ level (moderate signal) and (b) the vibrationless level (strong signal).

TABLE III. Collision-free lifetimes and level quenching rate constants for individual vibronic levels of the ^1A_u state of glyoxal.

^1A_u level	Wavelength[a] (Å) Excite (band)	Observe (band)	Lifetime (μsec)	Quenching rate constant[b] (10^{-10} cm^3 sec^{-1})
0	4552 (0–0)	4778 (8_1^0)	2.41 ± 0.06	1.78 ± 0.10
7^1	4528 (7_1^1)	4754 ($8_1^0 7_1^1$)	2.38 ± 0.07	4.5 ± 0.3
7^2	4507 (7_2^2)	4456 (7_0^2)	2.52 ± 0.08	6.0 ± 0.4
7^3	4435 (7_1^3)	4485 (7_3^3)	2.45 ± 0.08	6.3 ± 0.4
7^4	4414 (7_2^4)	4464 (7_4^4)	2.38 ± 0.14	6.6 ± 0.5
5^1	4447 (5_0^1)	4559 (5_1^1)	2.13 ± 0.05	3.2 ± 0.2
$5^1 7^1$	4426 ($5_0^1 7_1^1$)	4537 ($5_1^1 7_1^1$)	2.09 ± 0.06	2.4 ± 0.2
$5^1 7^2$	4406 ($5_0^1 7_2^2$)	4464 ($5_1^1 7_0^2$)	1.92 ± 0.07	2.9 ± 0.2
$5^1 7^3$	4385 ($5_0^1 7_3^3$)	4337 ($5_0^1 7_1^3$)	1.73 ± 0.08	6.6 ± 0.7
8^1	4403 (8_0^1)	4616 (8_1^1)	0.87 ± 0.03	5.8 ± 0.4
$8^1 7^1$	4383 ($8_0^1 7_1^1$)	4594 ($8_1^1 7_1^1$)	0.89 ± 0.03	7.9 ± 0.6
$8^1 7^2$[c]	4362 ($8_0^1 7_2^2$)	4314 ($8_0^1 7_0^2$)	1.49 ± 0.07	8.3 ± 0.7
$8^1 7^3$[c]	4342 ($8_0^1 7_3^3$)	4295 ($8_0^1 7_1^3$)	1.28 ± 0.06	8.2 ± 0.7
4^1	4360 (4_0^1)	4573 (4_1^1)	1.51 ± 0.05	6.0 ± 0.4
$4^1 7^1$	4341 ($4_0^1 7_1^1$)	4551 ($4_1^1 7_1^1$ & $4_0^1 8_1^0 7_1^1$)	1.55 ± 0.06	3.8 ± 0.4
$4^1 7^2$	4321 ($4_0^1 7_2^2$)	4274 ($4_1^1 7_0^2$)	1.43 ± 0.08	7.1 ± 0.7
$4^1 7^3$	4301 ($4_0^1 7_3^3$)	4255 ($4_0^1 7_1^3$)	1.57 ± 0.08	9.5 ± 0.8
2^1	4279 (2_0^1)	4625 (2_1^1)	1.43 ± 0.04	6.3 ± 0.3
$2^1 7^1$	4260 ($2_0^1 7_1^1$)	4602 ($2_1^1 7_1^1$)	1.37 ± 0.05	7.3 ± 0.6
$2^1 7^2$	4241 ($2_0^1 7_2^2$)	4196 ($2_0^1 7_0^2$)	1.58 ± 0.08	11.0 ± 0.9
$2^1 7^3$	4222 ($2_0^1 7_3^3$)	4177 ($2_0^1 7_1^3$)	1.70 ± 0.11	12.4 ± 1.0
$4^1 5^1$[d]	4266 ($4_0^1 5_0^1$)	4582 ($4_1^1 5_1^1$)	1.44 ± 0.06	5.3 ± 0.5
8^2[d]	4263 (8_0^2)	4681 (8_2^2)	0.78 ± 0.03	7.2 ± 0.8
$8^2 7^1$[d]	4246 ($8_0^2 7_1^1$)	4661 ($8_2^2 7_1^1$)	1.01 ± 0.06	7 ± 1
$8^1 4^1$[d]	4227 ($8_0^1 4_0^1$)	4426 ($8_1^1 4_0^1$ & $8_0^1 4_1^1$)	0.87 ± 0.04	7.0 ± 1.7
$2^1 8^1$[d]	4145 ($2_0^1 8_0^1$)	4545 ($2_0^1 8_2^1$)	0.82 ± 0.03	8.1 ± 1.0

[a]Wavelengths ±1 Å.
[b]Rate constants are for observation with 10 Å bandpass and ~0.5 Å excitation bandwidth (see text).
[c]These results may include significant contributions from $4_0^1 7_y^x$ transitions in both excitation and fluorescence.
[d]Previously unidentified level assigned on basis of predicted location.

These low pressure values all agree well with the extrapolated values.

IV. RESULTS

The measured collision-free lifetimes are given in Table III and plotted in Fig. 4 as a function of excess vibrational energy in the ^1A_u state. The error limits given in Table III for the lifetime values are the sum of the effect of time resolution and pressure measurement errors, estimated to be 2%, plus two standard deviations from the least-squares fit to the data. Except for the $8^1 7^2$ and $8^1 7^3$ levels, possible errors resulting from hot bands and overlapping bands are much less than the quoted uncertainty. Approximate error bars for the lifetime values are shown in Fig. 4.

The self-quenching rate constants for the individual vibrational levels are also given in Table III and plotted in Fig. 5. Since these rate constants are more affected by errors in pressure measurement, including impurities, than are the lifetimes, the estimated error from this source is 3% of the observed value. The time resolution uncertainty is approximately 1%. Therefore the error limits adopted for the quenching rate constants as given in Table III are 4% plus two standard deviations from the least-squares fit to the data.

V. DISCUSSION

A. Collision-free lifetimes

The collision-free lifetime measurements are of interest as a study of radiationless transition rates. However, it is difficult to draw direct conclusions from these data since there exists the possibility of substantial variations in the radiative lifetimes of the various vibrational levels. As mentioned earlier, ν_8, for example, has a vibronic interaction that is significant due to the relatively weak ^1A_u–^1A_g transition. Additionally, the possible effects of Franck–Condon factors on the radiative decay rates are unknown. One cannot assume that all observed differences are due to nonradiative processes, and quantum yield data which do not now exist are required to separate the radiative and nonradiative decay rates.

The most intriguing lifetime result is that of the significantly shorter lifetime of the 8^1 level, the only vibrational mode of glyoxal with b_g symmetry. It has been shown[23] that ν_8 can promote intersystem crossing from the ^1A_u to the ^3A_u state, providing an extra loss channel from levels such as 8^1. However, it has been observed[24] that there is no appreciable ^3A_u–^1A_g phosphorescence at pressures below 1 mTorr. Hence no additional intramolecular loss to the ^3A_u state is expected. The vibronic shortening of the radiative lifetime is expected to be important. However, even if the 8_1^1 and 8_0^1 bands equaled the 0–0 band in intensity, this vibronic interaction would not provide a sufficient decrease in the radiative lifetime of the 8^1 level to account for the observed lifetime value. We conclude that most of the additional loss from this level is due to internal conversion to the ^1A_g state.

The torsional mode exhibits an approximately constant lifetime over a range of about 900 cm^{-1} of excess energy in the ^1A_u state, a result characteristic of small molecules. As a well-behaved set of lifetime values, this series provides a striking contrast with other vibrational modes of glyoxal.

The third series of interest is the vibrationless level and the 5^1, 4^1, and 2^1 levels which show a systematic decrease in lifetime as vibrational energy increases. All of these are of the same a_g symmetry. While this behavior is similar to that of large molecule radiationless transitions, the possible effects of anharmonicity or frequency changes between the states may well be more significant than the change in density of states over this limited energy range. At the current level of development of radiationless transition theory, one cannot assess the importance of either of these parameters. Effects due to Franck–Condon factors on either radiative or nonradiative decay of glyoxal are unknown. While no definite conclusions can be made, we believe that the observed variations in lifetimes are dominated by internal conversion from the ^1A_u state to the ^1A_g state.

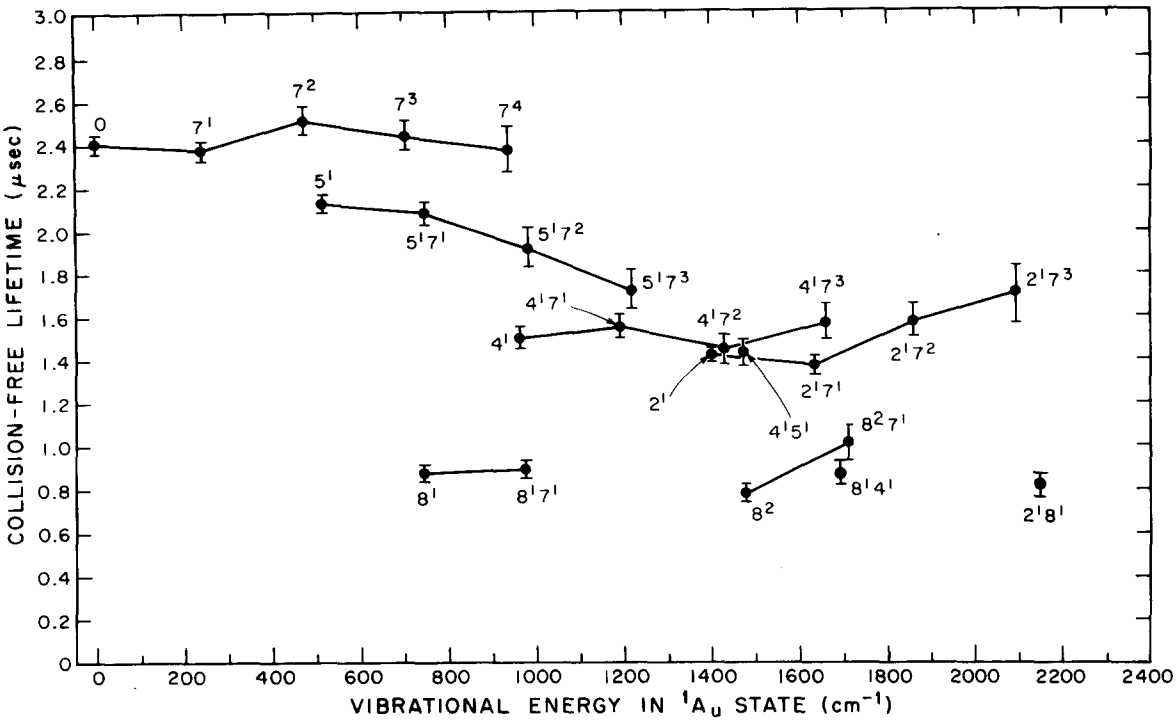

FIG. 4. Collision–free lifetimes for individual vibrational levels of the ^1A_u state of glyoxal.

B. Single vibronic level loss rate constants

The rate constants reported here for quenching of single vibrational levels are interpreted as being the sum of collisional vibrational relaxation, collision induced intersystem crossing, and collision induced internal conversion. For glyoxal molecules in the ^1A_u state, experimental evidence[24,25] suggests the first two are the most important mechanisms.

These rate constants are interesting in particular for their indication of long-range glyoxal–glyoxal interac-

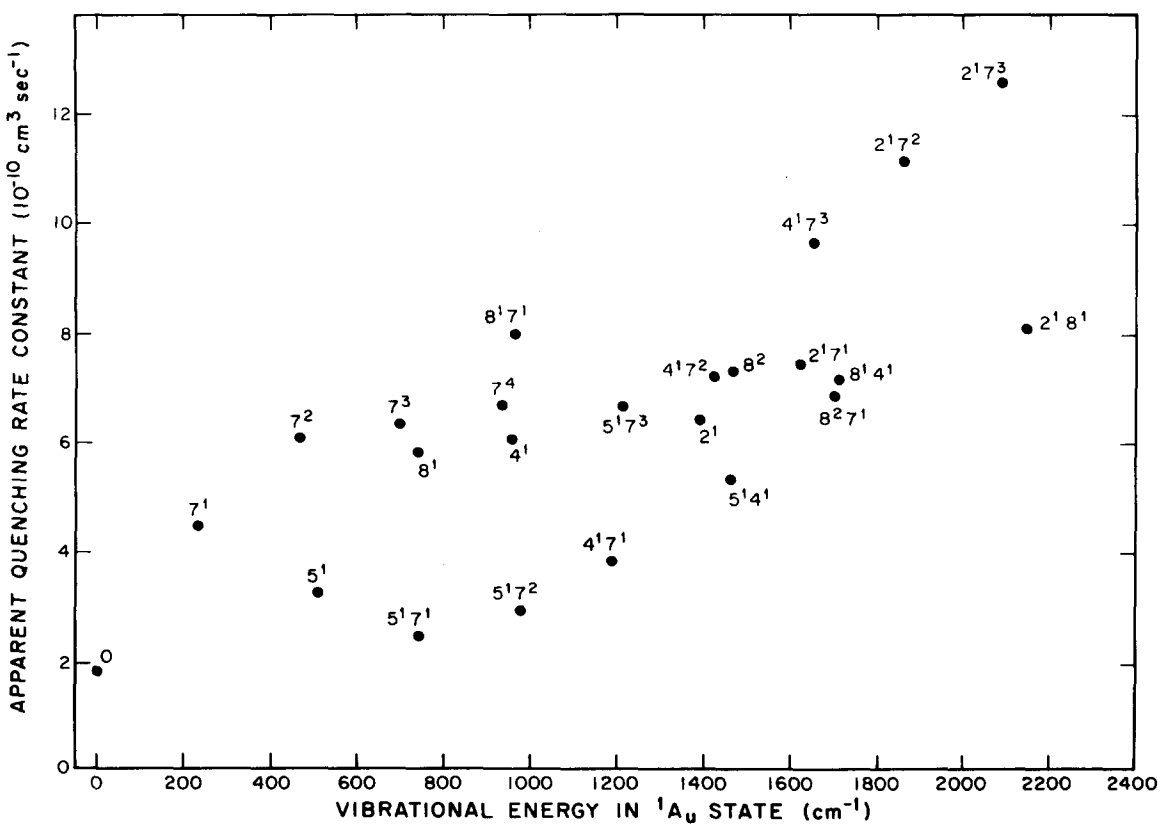

FIG. 5. Rate constants for quenching of single vibrational levels of the ^1A_u state of glyoxal by ground state glyoxal molecules.

tions. For comparison, a rate constant of about 2.3×10^{-10} cm^3 sec^{-1} corresponds to the hard-sphere gas kinetic collision rate for glyoxal–glyoxal collisions. One may also observe that the Stern–Volmer quenching plots are obtained over a pressure regime that might normally be considered collision-free for a 4 Å hard-sphere molecule. As shown in Fig. 5, there is also a general trend towards faster loss with increasing energy in the ^1A_u state, as the number of nearby vibronic levels increases. The rate constants vary from slightly less than gas kinetic to about seven times gas kinetic, assuming a 4 Å molecular diameter. It will be shown later[21] that these rate constants are in fact dominated by vibrational relaxation within the ^1A_u state.

The long-range glyoxal–glyoxal forces are also manifest in processes other than vibrational relaxation. In a study of ^3A_u–^1A_g phosphorescence, it has been observed[24,25] that collision-induced intersystem crossing from the ^1A_u state to the ^3A_u state can be observed at pressures as low as 3 mTorr. At this pressure the ^1A_u lifetime is 2 μsec, compared to a 35 μsec hard-sphere collision time. The geometry of glyoxal suggests that forces similar to hydrogen-bonding forces are present to some extent. This same intermolecular attraction may be related to the rapid formation of glyoxal polymer[20] at higher pressures. Thus the presence of additional glyoxal–glyoxal forces as manifest in the rate constants given here is not unexpected.

C. Comparison with previous work

Two previous time-resolved studies of the ^1A_u state of glyoxal utilizing dye-laser excitation of the 0–0 absorption band and extrapolation to zero pressure of the quenching plots have been reported. In the first of these, Yardley *et al.*[10] found the collision-free lifetime of the vibrationless level to be (2.18 ± 0.05) μsec. More recently Beyer and Lineberger[26] reported a value of (2.17 ± 0.02) μsec for this level. These values differ significantly with the value of (2.41 ± 0.06) μsec reported here.

The principal differences between the earlier work and the present observations are the pressure range of the measurements and the observational bandpass. It is not expected that the excitation bandwidth differences are important for the vibrationless level. In the report of Yardley *et al.*,[10] the fluorescence is viewed through long-pass filters that cut on at 4700 or 5000 Å. Glyoxal pressures range from ~3 to 1000 mTorr. Under these experimental conditions, rapid vibrational relaxation[21] and wide observational bandwidth can combine to produce an average lifetime of some group of vibrational levels. However, the relative populations of these levels may be a function of pressure. Combined with the cut-on filter bandpass, it is difficult to make a precise comparison with the present results.

In the work of Beyer and Lineberger,[26] the pressure range 40–150 mTorr was still too high to avoid major effects due to vibrational relaxation. However, the use of a spectrometer to resolve emission made possible the detection of the presence of the relaxation effects. The value reported in the present work is obtained if the curve of Beyer and Lineberger[26] is extended to lower pressure; i.e., due to the vibrational relaxation in the ^1A_u state the quenching plot is nonlinear. At low pressures a slope of 5.8 μsec^{-1} · Torr^{-1} is observed with 10 Å bandpass while at high pressures (> 40 mTorr) a curve with slope near 1.9 μsec^{-1} · Torr^{-1} is observed.

The value presented here for the lifetime of the vibrationless level is therefore more reliable than the previous reports due to the combination of low glyoxal pressure and spectrometer resolution of the emission to eliminate the effects due to vibrational relaxation. In addition, it also agrees with a lifetime measured under good signal-to-noise conditions at a pressure near 10^{-5} Torr with the same apparatus. It is interesting to note that Yardley *et al.*[10] used a similar low pressure reading (3.7 mTorr thermocouple reading) to substantiate their extrapolated value. However, no evaluation of this datum is possible without further experimental details.

Although no attempt was made in the present experiment to duplicate the work of Yardley *et al.*[10] explicitly, the emission has been observed broadband (1P28/V1 photomultiplier response limited). Over a pressure range from a few mTorr to several Torr the quenching curve is linear with a slope of (2.1 ± 0.1) μsec^{-1} · Torr^{-1} and gives a zero-pressure extrapolated lifetime of (2.5 ± 0.2) μsec. The principal difficulty with this observational method is that scattered laser light is dominant at early times and fluorescence decay may be observed only during a time when vibrational relaxation may be important at the lower pressures.

Yardley has also reported[11] a zero pressure lifetime of 2.24 μsec for the vibrationless level of the ^1A_u state. Frad and Tramer[27] report lifetimes of ~0.8 μsec for the 8^1 level and 2.04 μsec for the vibrationless level. Since no details have yet been published it is difficult to compare these values with the present results. No values for other levels of the ^1A_u state of glyoxal have been found in the literature. As noted earlier, the quenching rate constants are a strong function of excitation and observational bandwidth. Therefore no attempt has been made to compare the present results with the few numbers available in the literature.

VI. CONCLUSION

Collision-free lifetimes have been presented for 26 single vibrational levels of the ^1A_u state of glyoxal. Although quantitative rates for nonradiative decay of these levels cannot be determined without quantum yield values, the range of variation is suggestive of significant differences in the nonradiative decay. Since other observations show that production of the ^3A_u state from the ^1A_u state takes place primarily through collisions, the principal path of nonradiative decay is expected to be to the ^1A_g ground state. The magnitude of the decay rates also has been shown to be dependent on parameters other than symmetry of the vibrational mode in at least some cases. It is expected that with the availability of quantum yield values these lifetimes will provide a valuable test of radiationless transitions theory.

Rate constants for the quenching of these levels by

ground state glyoxal molecules are also reported. These rate constants give a clear demonstration of long-range glyoxal–glyoxal forces and extremely rapid vibrational relaxation in the ^1A_u state.

ACKNOWLEDGMENTS

The authors wish to thank Mr. Dennis Levin who very ably set up the data acquisition and analysis program. Support by the National Science Foundation under Grant GP-33666 and by the Council on Research and Creative Work of the University of Colorado is gratefully acknowledged.

*Present address: U.S.A. Ballistic Research Laboratories, Aberdeen Proving Ground, Maryland.
†Alfred P. Sloan Foundation Fellow.

[1]J. Jortner, S. A. Rice, and R. M. Hochstrasser, Adv. Photochem. 7, 149 (1969) and references therein.
[2]E. W. Schlag and H. von Weyssenhoff, J. Chem. Phys. 51, 2508 (1969).
[3]U. Laor and P. K. Ludwig, J. Chem. Phys. 54, 1054 (1971).
[4]H. von Weyssenhoff and F. Kraus, J. Chem. Phys. 54, 2387 (1971).
[5]E. S. Yeung and C. B. Moore, J. Chem. Phys. 58, 3988 (1973).
[6](a) C. Guttman and S. A. Rice, J. Chem. Phys. 61, 661 (1974); (b) R. Scheps, D. Florida, and S. A. Rice , *ibid.* 61, 1730 (1974); (c) K. G. Spears and S. A. Rice, *ibid.* 55, 5561 (1971); (d) M. H. Hui and S. A. Rice, *ibid.* 61, 833 (1974), and references contained therein.
[7]A. Frad, F. Lahmani, A. Tramer, and C. Tric, J. Chem. Phys. 60, 4419 (1974).
[8]A. V. Pocius and J. T. Yardley, J. Chem. Phys. 61, 2779 (1974).
[9]J. Paldus and D. A. Ramsay, Can. J. Phys. 45, 1389 (1967) and references therein.
[10]J. T. Yardley, G. W. Hollman, and J. I. Steinfeld, Chem. Phys. Lett. 10, 266 (1971).
[11]J. T. Yardley, 26th Symposium on Molecular Structure and Spectroscopy, Columbus, Ohio (1971) (unpublished).
[12]H. L. McMurry, J. Chem. Phys. 9, 241 (1941).
[13]G. Herzberg, *Molecular Spectra and Molecular Structure*, III (Van Nostrand, Princeton, 1967), p. 137ff.
[14]W. Holzer and D. A. Ramsay, Can. J. Phys. 48, 1759 (1970).
[15]B. W. Woodward, V. J. Ehlers, and W. C. Lineberger, Rev. Sci. Instrum. 44, 882 (1973).
[16]T. W. Hänsch, Appl. Opt. 11, 895 (1972).
[17]M. J. Bennett and F. C. Thomkins, Trans. Faraday Soc. 53, 185 (1957).
[18]P. B. Sackett, Appl. Opt. 11, 2181 (1972).
[19]H. L. Riley and N. A. C. Friend, J. Chem. Soc. 1932, 2342.
[20]R. G. W. Norrish and J. G. A. Griffiths, J. Chem. Soc. 1928, 2829.
[21]R. A. Beyer and W. C. Lineberger (to be published).
[22](a) O. Stern and M. Volmer, Phys. Z. 20, 183 (1919); (b) J. I. Steinfeld, Acc. Chem. Res. 3, 313 (1970).
[23]E. Drent and J. Kommandeur, Chem. Phys. Lett. 14, 321 (1972).
[24]R. A. Beyer and W. C. Lineberger (to be published).
[25]L. G. Anderson, C. S. Parmenter, and H. M. Poland, Chem. Phys. 1, 401 (1973).
[26]R. A. Beyer and W. C. Lineberger, Chem. Phys. Lett. 20, 600 (1973).
[27]A. Frad and A. Tramer, Chem. Phys. Lett. 23, 297 (1973).